17

Underwater Robots Part II: Existing Solutions and Open Issues

Lapierre Lionel
Laboratory of Informatics, Microelectronics and Robotics of Montpellier (LIRMM)
France

This paper constitutes the second part of a general overview of underwater robotics. The first part is titled: *Underwater Robots Part I: current systems and problem pose*. The works referenced as (Name*, year) have been already cited on the first part of the paper, and the details of these references can be found in the section 7 of the paper titled *Underwater Robots Part I: current systems and problem pose.* The mathematical notation used in this paper is defined in section 4 of the paper *Underwater Robots Part I: current systems and problem pose.*

1. Introduction

We propose in the sequel to introduce the existing solutions of the problems mentioned in the section 6 of the paper: *Underwater Robots Part I: current systems and problem pos*e. We will present the solutions that allows for guaranteeing the desired global performances exposed previously. Section 2 presents the solutions to the Modelling problems. Section 3 introduces the different navigation systems currently in used. Section 4 proposes an overview of the classic Guidance strategies, and point out the specificities of this Guidance system that allow solving various problems. Section 5 presents the Control solution, underlying the ones that exhibit guaranteed performances. The Mission Control, Software and hardware architectures problems will be briefly mentioned in section 6. Finally section 7 concludes this paper and section 8 presents de references used.

2. Naval architecture

This development assumes the *principle of superposition* that is, for most marine control application, a good approximation. These modelled phenomena are described in (Newmann, 1977), and for the most significant ones to underwater robotics, listed below.

2.1 Added Mass

The hydrodynamic forces due to added mass are a consequence of the kinetic energy exchanges between the system and the surrounding water. Consider an object moving with a strictly positive acceleration with respect to the surrounding fluid. The energy expense of the system is caused by the system inertial forces, and the inertial forces of the surrounding particles of water that has to be compensated in order to induce the movement. Thus, added

Source: Mobile Robots Towards New Applications, ISBN 3-86611-314-5, Edited by Aleksandar Lazinica, pp. 784, ARS/plV, Germany, December 2006

mass has an inertial incidence, as the system mass itself. In a situation of a strictly negative acceleration with respect to the surrounding fluid, the moving water particles will restore their kinetic energy to the system. The consequence is that the global apparent mass of an immerged object is bigger than its intrinsic- (or dry-) mass.
Notice that the added mass effect is a function of the fluid characteristics, the system geometry, and the body-frame-direction of the acceleration. Then, an immerged system will not have the same inertial behaviour – apparent mass – in all the directions, in opposition to the classic fundamental equation of the dynamics ($F = m \cdot a$), where the mass is not a function if the direction of the acceleration.
Moreover, the added mass forces are applied logically at the centre of gravity of the surrounding moving water. This point coincides with the system buoyancy centre, function of its geometry, while the dry-inertial effects impacts on the system centre of gravity.
The contribution from this added mass phenomena are mathematically expressed as:

$$\boldsymbol{\tau}_{\mathbf{A}} = -\mathbf{M}_{\mathbf{A}}\dot{\boldsymbol{\nu}} - \mathbf{C}_{\mathbf{A}}(\boldsymbol{\nu}) \cdot \boldsymbol{\nu}$$

As for the rigid body dynamics, it is advantageous to separate the added mass forces and moments in terms which belong to the added mass system 6x6 inertia matrix $\mathbf{M}_{\mathbf{A}}$ and the 6x6 matrix of hydrodynamic Coriolis and centripetal terms denoted $\mathbf{C}_{\mathbf{A}}(\boldsymbol{\nu}) \cdot \boldsymbol{\nu}$. To derive the expression of these two matrices, an energy approach based on Kirchhoff's equations is applied. The reader will find in (Fossen, 2002) and (Newmann, 1977) the detailed background material in order to estimate the added mass coefficients of a given object shape.

2.2 Hydrodynamic Damping

D'Alambert's paradox states that no hydrodynamic forces act on a solid moving completely submerged with constant velocity in a non-viscous fluid. In a viscous-fluid, frictional forces are present such that the system is not conservative with respect to energy (Fossen, 2002).
An object, immerged in a viscous fluid flow undergoes a force due to the relative velocity fluid/object, which can be decomposed with a component along the velocity direction, *the drag*, and a perpendicular second component, *the lift*, as depicted in Fig. 1. The origin of these forces is the non-isotropic repartition of the pressure around the object. Notice that a spherical or cylindrical object will only undergo a drag effect, since this geometry induces a symmetrical flow separation whatever the relative flow direction. Hence, for ROV-type vehicle, where isotropy is a sought factor, the lift effect is generally neglected. In the case of AUV-type vehicle, the control surfaces are using the lift effect to create a change in the direction of the robot velocity with respect to the fluid flow. Nevertheless, the main body of the AUV generally exhibits planes of symmetry that justify neglecting the lift effect. Thus, lift effect is generally modelled and considered in the actuation model, in order to evaluate the control surfaces action. The drag and lift effect are modelled as follows:

$$L = \frac{1}{2} \cdot \rho \cdot C_L \cdot A(\alpha) \cdot |v_t| \cdot v_t$$

$$D = \frac{1}{2} \cdot \rho \cdot C_D \cdot A(\alpha) \cdot |v_t| \cdot v_t$$

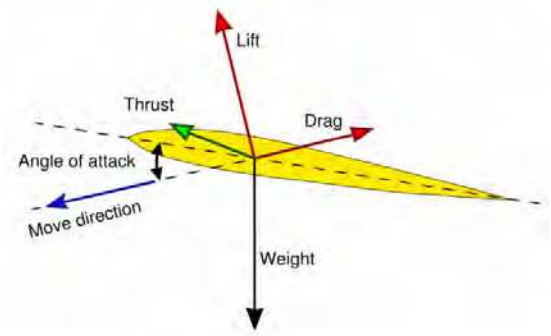

Fig. 1. Lift and Drag effects.

where L and D denote the lift and drag forces, respectively, ρ is the water density, α is the angle of attack, $A(\alpha)$ is the projected area perpendicularly to the flow direction and v_t is the relative fluid / object velocity. C_L and C_D are the lift and drag coefficients, respectively. These coefficients depends of the *Reynold number* of the immerged object, which is a function of the object geometry, the fluid density and the relative velocity, (Goldstein, 1976). The drag effect, as previously described is in fact the most significant hydrodynamic damping undergone by a robotics underwater system, and is specifically called *pressure drag*. Other damping related phenomena exist. The *skin friction* is due to the water viscosity and the object surface roughness. It induces a water 'sticking' effect that engenders a small drag phenomenon. This is generally neglected in the scope of underwater robotics applications. The *wave drift damping* can be interpreted as added resistance for surface vessels advancing in waves. Notice that, as stated for the added mass, the point of application of these forces is the system buoyancy centre. The reader will find in (Faltinsen, 1995) and (Newmann, 1977) detailed material to estimate the *Reynold number* and drag and lift coefficients.
Finally, the drag expressions acting on the 6 degrees of freedom of the solid are written as $\mathbf{D}(\mathbf{v})\cdot\mathbf{v}$, where $\mathbf{D}(\mathbf{v})$ is the 6×6 system damping matrix.

2.3 Restoring Forces

Beside the mass and damping forces, underwater systems and floating vessels will also be affected by gravity and buoyancy forces. In hydrodynamic terminology, the gravitational and buoyancy forces are called *restoring forces*, and they are equivalent to the spring forces in a *mass-spring-damper* system (Fossen, 2002). The gravity force or system weight, $W = \rho g$, where m denotes the system mass and g the acceleration of gravity, acts at the system gravity centre. The buoyancy force is expressed as $W = \rho \cdot g \cdot \nabla$ where ρ is the water density and ∇ is the volume of fluid displaced by the vehicle, and is applied at the volumetric centre (equivalently called buoyancy centre) of the displaced fluid. Notice that for a fully immerged solid the buoyancy centre coincides with the volumetric centre of the solid. Let $\mathbf{r}_g = [x_g \quad y_g \quad z_g]^T$ and $\mathbf{r}_b = [x_b \quad y_b \quad z_b]^T$ define the location of the gravity and buoyancy centres with respect to the origin of the body-frame {B}, respectively. Then, the 6×1 vector $\mathbf{G}(\boldsymbol{\eta})$ expressing the restoring forces along the 6 degrees of freedom of the system can be written as in equation (2).

$$\mathbf{G}(\boldsymbol{\eta}) = \begin{bmatrix} (W-B)\cdot\sin\theta \\ -(W-B)\cdot\cos\theta\cdot\sin\phi \\ -(W-B)\cdot\cos\theta\cdot\cos\phi \\ -(W\cdot y_g - B\cdot y_b)\cdot\cos\theta\cdot\cos\phi + (W\cdot z_g - B\cdot z_b)\cdot\cos\theta\cdot\sin\phi \\ (W\cdot z_g - B\cdot z_b)\cdot\sin\theta + (W\cdot x_g - B\cdot x_b)\cdot\cos\theta\cdot\cos\phi \\ -(W\cdot x_g - B\cdot x_b)\cdot\cos\theta\cdot\sin\phi - (W\cdot y_g - B\cdot y_b)\cdot\sin\theta \end{bmatrix} \quad (2)$$

In addition to the restoring forces $\mathbf{G}(\boldsymbol{\eta})$, the system can be equipped with ballasts allowing for pumping water in order to modify the system weight, and as a consequence, the location of the gravity centre. Hence $\mathbf{r}_g$ and W become controllable variables that allows for heave, pitch and roll dynamic stabilisation, for surface or semi-submersible vessels, depending on the number and the location of the ballast tanks (Faltinsen, 1995). Notice that underwater Glider systems are using this ballast control to alternate a the gravity / buoyancy dominancy in order to create a descending / ascending forces that induce a water flow in which the system flies.

2.4 Environmental disturbances

Environmental disturbances, due to waves, wind and ocean currents have a significant impact on marine system dynamics. Simple models for these disturbances applicable to control system design are found in (Fossen, 2002) and (Prado, 2004). A more general discussion on marine hydrodynamics is presented in (Faltinsen, 1995) and (Newmann, 1977). Notice that wave and wind effects have an effective incidence on surface and sub-surface ASCs, and UUVs shallow water application.

Winds affect surface vessels and their consideration is necessary for designing large crude carriers and tankers auto-pilots. ASCs are generally designed in such a way that wind resistance is negligible, but (Neal, 2006) is presenting an interesting study on a small-scaled sailing ASC and demonstrates the feasibility and interest of such a system.

Waves are induced by many factors: wind, tide, storm surges and *Stokes* drift. A linear propagating wave theory is derived, borrowing from potential theory and Bernouilli's equations. It allows for a statistical description of wave based on an estimated wave spectrum. The wave elevation, ξ_z, of a long-crested irregular sea propagating along the positive x-axis can be written as the sum of a large number of wave components, i.e.:

$$\xi_z = \sum_{j=1}^{n} A_j \cdot \sin\left(\omega_j \cdot t - k_j \cdot x + \varepsilon_j\right)$$

Where A_j, ω_j, k_j and ε_j are respectively the wave amplitude, circular frequency, wave number and random phase angle of wave component *j*. The random phase angles ε_j are uniformly distributed between 0 and 2π and constant with time. The wave amplitude A_j is distributed according to a wave spectrum estimated from wave measurements. Recommended sea spectra from ISCC (International Ship and Offshore Structures Congree) and ITTC (International Towing Tank Conference) are often used to calculate A_j (Faltinsen, 1995). Underwater, ω_j and k_j are related with a dispersion relationship that rapidly attenuates the wave effects with depth. This attenuation effect is clearly stated in the expression of the horizontal fluid velocity $\dot{\xi}_x$ and acceleration $\ddot{\xi}_x$:

$$\dot{\xi}_x = \sum_{j=1}^{n} \omega_j \cdot A_j \cdot e^{-k_j z} \sin\left(\omega_j \cdot t - k_j \cdot x + \varepsilon_j\right)$$

$$\ddot{\xi}_x = \sum_{j=1}^{n} \omega_j^2 \cdot A_j \cdot e^{-k_j z} \cos\left(\omega_j \cdot t - k_j \cdot x + \varepsilon_j\right)$$

The wave-induced velocity and acceleration vectors of the surrounding particles of fluid are expressed as $\dot{\boldsymbol{\xi}}$ and $\ddot{\boldsymbol{\xi}}$.

The wave-induced oscillatory disturbance is rapidly attenuated with the depth, and in most UUVs application is neglected. But, ocean current is more problematic. Ocean current are horizontal and vertical circulation systems of ocean waters produced by tides, local wind, *Stokes* drift major ocean circulation, storm surges and strong density jumps in the upper ocean (combined action of surface heat exchange and salinity changes). As for the wave effect, ocean current induces on an immerged object a hydrodynamic load, due to the externally-induced movement of the surrounding particles of water. The low dynamic of the phenomena justifies assuming that the current is slowly-varying, hence the current velocity vector ς, expressed in the universal frame {*U*} is considered as constant.

Then the wave and ocean current induced disturbances are modelled as the universal velocity $\boldsymbol{\nu}_{\mathbf{w}}$ and acceleration $\dot{\boldsymbol{\nu}}_{\mathbf{w}}$ of the surrounding fluid. Expressed in the body frame {*B*}, it comes:

$$\boldsymbol{\nu}_{\mathbf{w}} = \mathbf{R} \cdot \left(\dot{\boldsymbol{\xi}} + \varsigma\right)$$

$$\dot{\boldsymbol{\nu}}_{\mathbf{w}} = \mathbf{R} \cdot \ddot{\boldsymbol{\xi}} + \dot{\mathbf{R}} \cdot \left(\dot{\boldsymbol{\xi}} + \varsigma\right)$$

Finally, considering the previously described environmental disturbances, the external disturbances acting on an immerged vehicle are expressed by the 6×1 vector **w**:

$$\mathbf{w} = \mathbf{M}_A(\boldsymbol{\eta}) \cdot \dot{\boldsymbol{\nu}}_w + \mathbf{C}_A(\boldsymbol{\nu}_w) \cdot \boldsymbol{\nu}_w + \mathbf{D}(\boldsymbol{\nu}_w) \cdot \boldsymbol{\nu}_w$$

Considering the superposition principle, this formalism allows for modelling the hydrodynamic forces that the system will undergo, in function of the system states $\boldsymbol{\eta}$ and $\boldsymbol{\nu}$. A Newton-Euler analysis or a Lagrangian-type derivation allows for writing the equations of motion for an underwater robot without manipulator as follows (Fossen, 2002) and (Lapierre *et al.*, 1998):

$$\begin{aligned} \dot{\boldsymbol{\eta}} &= \mathbf{K}(\boldsymbol{\eta}) \cdot \boldsymbol{\nu} \\ \mathbf{M}(\boldsymbol{\eta}) \cdot \dot{\boldsymbol{\nu}} + \mathbf{C}(\boldsymbol{\nu}) \cdot \boldsymbol{\nu} + \mathbf{D}(\boldsymbol{\nu}) \cdot \boldsymbol{\nu} + \mathbf{G}(\boldsymbol{\eta}) &= \boldsymbol{\tau} + \mathbf{w} \\ \boldsymbol{\tau} &= \mathbf{B} \cdot \mathbf{u} \end{aligned} \tag{3}$$

where the kinematic relation is written as:

$$\mathbf{K}(\boldsymbol{\eta}) = \begin{bmatrix} \cos\psi \cdot \cos\theta & -\sin\psi \cdot \cos\phi + \cos\psi \cdot \sin\theta \cdot \sin\phi & \sin\psi \cdot \sin\phi + \cos\psi \cdot \sin\theta \cdot \cos\phi & 0 & 0 & 0 \\ \sin\psi \cdot \cos\theta & \cos\psi \cdot \cos\theta + \sin\psi \cdot \sin\theta \cdot \sin\phi & -\cos\psi \cdot \sin\phi + \sin\psi \cdot \sin\theta \cdot \cos\phi & 0 & 0 & 0 \\ -\sin\theta & \cos\theta \cdot \sin\phi & \cos\theta \cdot \cos\phi & 0 & 0 & 0 \\ 0 & 0 & 0 & 1 & \sin\phi \cdot \tan\theta & \cos\phi \cdot \tan\theta \\ 0 & 0 & 0 & 0 & \cos\phi & -\sin\phi \\ 0 & 0 & 0 & 0 & \dfrac{\sin\phi}{\cos\theta} & \dfrac{\cos\phi}{\cos\theta} \end{bmatrix} \tag{4}$$

M denotes the 6x6 symmetric inertia matrix as the sum of the diagonal rigid body inertia matrix and the hydrodynamic added mass matrix $\mathbf{M_A}$, **C(v)** is the 6×6 Coriolis and centripetal matrix including rigid-body terms and terms $\mathbf{C_A(v)}$ due to added mass, D(v) is the 6×6 damping matrix

including terms due to drag forces, $\mathbf{G}(\boldsymbol{\eta})$ is a 6x1 vector containing restoring terms formed by the vehicle buoyancy and gravitational terms and $\mathbf{w}$ is the 6x1 vector representing the environmental forces and moments (e.g. wave and current) acting on the vehicle.
The actuation input $\mathbf{u}$ is composed with the thrusters' propeller angular velocity and the desired angle of the control surfaces. Thrusters' dynamics are nonlinear and quite complex. The reader will find in (Yuh, 2000), (Whitcomb and Yoerger, 1995), and the references therein, experimental elements to compare four thrusters models for blade-propeller type underwater thrusters driven by brushless DC motor. Control surfaces are using the lift effect to act on the system. Approximated theoretical solutions and experimental data have been collected to produce efficient models reported in (Fossen, 2002) and (Aucher, 1981). Notice that Equation (3) expresses a linear relation between $\boldsymbol{\tau}$ and $\mathbf{u}$. This approximation is justified under the assumption that the thruster's dynamics have much smaller time constants than the vehicle dynamics [YUH]. Nevertheless, for control surfaces neglecting second order terms might be far from reality. Moreover, control surfaces are undergoing heavy hydrodynamic reaction forces, inducing deformations and a decrease in the drive motor response.
The constant physical parameters of the actuation model compose the $\mathbf{B}$ matrix**.** Its components are dependent on each robot's configuration, control surfaces, ballast system, number and location of thrusters. Therefore $\mathbf{B}$ is generally not a diagonal, even square matrix.
The environmental disturbance, $\mathbf{w}$, induces a dynamic load on the system that can be considered during the control design, since many of these effects are suppressed in the closed loop. Moreover, ocean current induces on the system a static inertial-based load that modifies the working condition of thrusters and, as we will see later confronts an under-actuated system (ASC, AUV) with the Brocket's limitations (Brockett*, 1983) and impedes it to realize a pose stabilisation with a desired heading.
When one or more manipulators are attached to the vehicle, it becomes a multi-body system and modelling becomes more complicated. The effects of the hydrodynamics on each link of the manipulators on vehicle motion have to be considered. Moreover, underwater manipulation requires the manipulator end-effector to exert a desired force on the structure on which the intervention is performed. Hence, the modelling has to explicitly consider the effects of the environment reaction on the system. Using the fact that intervention is done while the vehicle is station-keeping, the system model is simplified and decoupled (Whitcomb*, 2000), (Lapierre[a] *et al.*, 1998) and (Fraisse *et al.*, 2000).

2.5 Biological Inspired system: theory of locomotion

During a movement, fishes are continuously adjusting their body-shape in order to locally control the fluid flow along their body, hence reaching high efficiency in the thrust generation. This continuous deformation is difficult to model, and general modelling solutions consider a hyper-redundant N-serially-linked segments system. The purpose of the dynamic model is to express the actuation effects on the system states evolution. Then, the control analysis allows for designing an actuation pattern (also called *gait*) that "wiggles" the body surface in order to generate the desired thrust. The relationship between shape and position changes requires mathematical analysis borrowing from fluid potential theory and Lie algebra (Sfakiotakis & Tsakiris, 2004). Notice the use of Lagrange multiplier technique with tensor notation, to obtain a solution of the dynamic model of an eel-like system (McIsaac & Ostrowski, 2002).

The physical constant parameters of the dynamic model (2) can be estimated using graphics in the literature. The dynamic parameters can also be precisely identified with hydrodynamic Tank Tests, reproducing an artificial fluid flow on the immerged structure, connected to a force sensor that allows for measuring the 6 forces and torques induced by the flow. Nevertheless, despite the precision of the model-parameters estimation, the modelling error has a significant impact on the control performances. Let $\mathbf{P}$ be the vector of the system dynamic parameters, $\hat{\mathbf{P}}$ is an estimation of $\mathbf{P}$ and $\tilde{\mathbf{P}} = \mathbf{P} - \hat{\mathbf{P}}$ denotes the modelling error. The control robustness denotes the system ability to react as desired, despite $\tilde{\mathbf{P}}$. Moreover, the previous modelled phenomena expressions assume that the neglected high order terms induce minor effect. This might be empirically verified, but the theoretical consideration of the effects of the *unmodelled dynamics* is still an opened issue. This unmodelled dynamics has also another interest. Indeed, an accurate modelling that explicitly considers the high order terms will result in a precise description of the system dynamics, allowing for fine simulations. Nevertheless, modelling does not imply controllability, and as we will see in the sequel, the control design will impose to neglect some problematic coupled and non-linear terms of the model.

3. Navigation System

The Navigation System provides estimates of the vehicle states based on a set of motion sensor suites.
As underwater systems have been developed, the complexity of the navigation problem increased. The demands are different in function of the system application. An ASC is riding the sea surface, and the navigation problem is to constantly estimate its global position with respect to the pre-defined geo-referenced route. The possibility to directly use GPS information and long-range radio link greatly simplifies the problem. A ROV navigation system will be tasked with estimating the necessary information in order to insure a robust and precise hovering control in front of the target on which the manipulation is performed. The approach phase requires similar information than for AUV, in order to control the system movement on a globally-defined or terrain-based route. Then, the navigation problem for UUVs is related with the estimation of the necessary information in order to accomplish the 3 following types of objectives:

- terrain-based pose-stabilisation ,
- terrain-based route following,
- globally-defined route following.

Underwater, the absence of direct GPS measurements leads different alternatives:

- periodic surfacing,
- pure dead-reckoning navigation,
- calibrated-acoustic-devices based navigation,
- terrain-based and SLAM navigation.

In any case, multiple sensors are needed in order to provide a set of sufficient measurements to estimate $\hat{\boldsymbol{\eta}}$ and $\hat{\boldsymbol{\nu}}$. UUV sensor suite is generally redundant, different sensors providing an estimation of the same physical quantity. Moreover, measurements related to the UUV movements are linked with the differential relation of the laws of mechanics. The navigation system is tasked with the fusion of these measurements in order to provide the best estimate of the system states.
As mentioned in (Pascoal *et al.*, 2000 and Oliveira, 2002) navigation system is traditionally done in a stochastic setting using *Kalman-Bucy* filtering theory (Brown & Hwang, 1992). The UUV situation

leads to consider nonlinear systems, and navigation solutions are usually sought by resorting to *Extended Kalman* filtering techniques. The stochastic setting requires a complete parameterization of process and observation noise, a task that may be difficult, costly, or not suited to the problem in hand. This issue is argued at length in (Brown & Hwang, 1972), where the author points out that in a great number of practical applications the filter design process is entirely dominated by constraints that are naturally imposed by the sensor bandwidth. In this case, a design method that explicitly addresses the problem of merging information provided by a given sensor suite over distinct, yet complementary frequency regions is warranted.

Complementary filters have been developed to address this issue explicitly (Oliveira, 2002). In the case where the navigation sensors can be sampled at the same period, the corresponding filter operators are linear and time-invariant. This leads to a fruitful interpretation of the filters in the frequency domain, as briefly described in Fig. 2, in the situation of heading estimation.

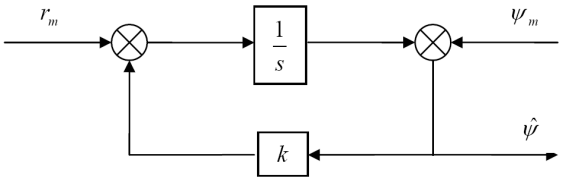

Fig. 2. complementary filter estimating the yaw angle $\hat{\psi}$ based on the measurements of the yaw-rate ψ_m and the yaw angle r_m, from (Pascoal *et al.*, 2000).

Straightforward computation allows for writing the filter structure of Fig. 2 as:

$$\hat{\psi}(s) = \underbrace{\frac{k}{s+k}}_{T_1(s)} \cdot \psi_m(s) + \underbrace{\frac{1}{s+k}}_{T_2(s)} \cdot r_m(s)$$

where the subscript $(\cdot)_m$ denotes the measurement, and $\hat{\psi}(s)$, $\psi_m(s)$ and $r_m(s)$ are the *Laplace* transform of $\hat{\psi}$, ψ_m and r_m, respectively. Notice the following important properties:

I $T_1(s)$ is low pass, the filter relies on information provided by the compass at low frequency only.

ii $T_2(s) = I - T_1(s)$. The filter blends the information provided by the compass in the low frequency region with that available form the rate gyro in the complementary region.

iii The break frequency is simply determined by the choice of the parameter k.

The frequency decomposition induced by the complementary filter structure holds the key of its practical success, since it mimics the natural frequency decomposition induced by the physical nature of the sensors themselves. Compasses provide reliable information at low frequency only, whereas rate gyros exhibit biases and drift phenomena in the same frequency region and therefore useful at higher frequencies. Complementary filter design is then reduced to the choice of k so as to meet a target break frequency that is entirely dictated by the physical characteristic of the sensors. From this point of view, this is in contrast with a stochastic approach that relies heavily on a correct description of process and measurement noise (Brown, 1972).

In the case of linear position, based on low-rate acoustically relayed global measurements, and acceleration estimation based on some onboard accelerometers, the navigation system

has to merge inertial frame position with body-axis accelerations. This explicitly introduces the nonlinear rotation matrix **R** from inertial to body-axis in the filter structure. The resulting nonlinear filter is cast in the framework of Linear Parametrically time-Varying systems (LPVs). Using this set-up, filter performance and stability are studied in an H_∞ setting by resorting to the theory of Linear Matrix Inequalities (LMIs, Boyd *et al.*, 1994).

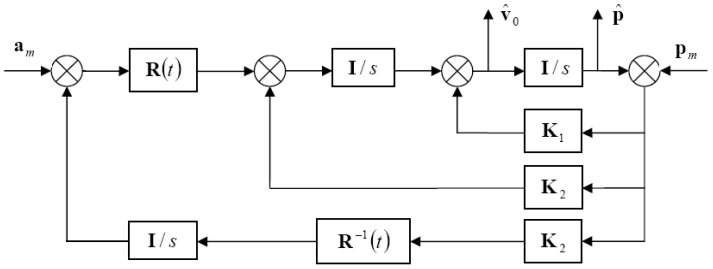

Fig. 3. complementary filter estimating the inertial position $\hat{\mathbf{p}}$ and velocity $\hat{\mathbf{v}}_0$ based on the measurements of the body-frame accelerations $\mathbf{a}_m$ and the inertial position $\mathbf{p}_m$ from (Pascoal ***et al.***, 2000).

Fig. 3 describes a filter that complements position information with that available from onboard accelerometers, where $\mathbf{a}_m = [\dot{u}_m \quad \dot{v}_m \quad \dot{w}_m]^T$ denotes the measured linear accelerations along the 3 body-axis, $\mathbf{p}_m = [x_m \quad y_m \quad z_m]^T$ is the measured absolute position, $\hat{\mathbf{v}}_0 = [\hat{\dot{x}} \quad \hat{\dot{y}} \quad \hat{\dot{z}}]$ is the inertial estimated velocity and $\hat{\mathbf{p}}$ is the estimated geo-referenced position. The structure design is then reduced to the choice of the gain matrices $\mathbf{K}_1$, $\mathbf{K}_2$ and $\mathbf{K}_3$. (Pascoal *et al.*, 2000) is converting the problem of filter design and analysis into that of determining the feasibility of the related set of Linear Matrix Inequalities. As a consequence, the stability of the resulting filters as well as their frequency-like performance can be assessed using numerical analysis tools that borrow from convex optimisation techniques (Boyd *et al.*, 1994 and Brown 1972).

Despite the time-varying problem, the characteristics of the sound channel imply that the position measurements are available at a rate that is lower than that of the velocity or acceleration sensors. To deal with this problem, (Oliveira, 2002) proposes an approach to navigation system design that relies on multi-rate *Kalman* filtering theory. Moreover, the author introduces some analysis tools to show that multi-rate filters can be viewed as input-output operators exhibiting "frequency-like" properties that are natural generalization of those obtained for the single rate case.

The filter of Fig. 3 proposes an interesting combination for the pose-stabilisation problem. Suppose a vision system providing an estimation of the relative position between a ROV and a visible landmark located on the structure onto which a manipulation has to be performed. The accelerometers and the vision system, equipped with appropriate feature extraction algorithms, provide precise necessary information to complete a hovering manoeuvre. (Kaminer *et al.*, 2001) provides the detailed solution to this problem, applied to the problem of estimating the relative position and velocity of an autonomous aircraft with respect to a moving platform, such as a naval landing vessel. This solution allows fusing accelerometers measurements with information coming from the image space, using an adequate vision system. The consequence is the injection in the filter structure of the vision

sensor model, as depicted in Fig. 4. **Fig. 4**, where $\mathbf{p}_m^{\mathrm{Im}}$ denotes the image coordinates of the desired feature, $\mathbf{R}_U^{Cam}(t)$ is the rotation matrix from the universal frame to the camera frame, h_θ is the calibrated vision-system model, expressing the relative position of the desired feature in the image frame $\mathbf{p}_m^{\mathrm{Im}}$ from the relative feature position expressed in the camera frame and H^T is the Jacobian matrix of h_θ.

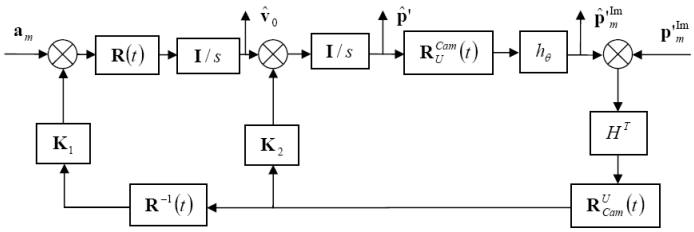

Fig. 4. complementary filter estimating the relative position of the desired feature with the UUV $\hat{\mathbf{p}}'$ and velocity $\hat{\mathbf{v}}_0$ based on the measurements of the body-frame accelerations $\mathbf{a}_m$ and the position of the desired feature in the image plane, $\mathbf{p}'^{\mathrm{Im}}_m$ from (Kaminer ***et al.***, 2001).

Moreover, the authors of (Kaminer *et al.*, 2001) show that the resulting filter exhibits guaranteed performances, that is:

$$\text{If } \left|\mathbf{p}'^{\mathrm{Im}}\text{-}\mathbf{p}'^{\mathrm{Im}}_m\right| < \zeta_p \text{ and } \left|\mathbf{a}\text{-}\mathbf{a}_m\right| < \zeta_a, \exists \boldsymbol{\varepsilon}, \text{such that } \tilde{\mathbf{p}}' = \mathbf{p}' - \hat{\mathbf{p}}' < \boldsymbol{\varepsilon}$$

where ζ_p is a bound on the measurement error, related with the sensor accuracy. The feasibility test, required for the choice of the gain matrices $\mathbf{K}_1$, $\mathbf{K}_2$ and $\mathbf{K}_3$, can be iterated order to minimize the guaranteed bound $\boldsymbol{\varepsilon}$, (Silvestre, 2000). An interesting unsolved question is related to the inverse problem: given a necessary $\boldsymbol{\varepsilon}$, what should be the sensors characteristics, in terms of sampling frequency and accuracy, that provide an estimation guaranteed to be within $\boldsymbol{\varepsilon}$.

A generalisation of the previous results allows to state that, given a complete sensor suite that provides $\boldsymbol{\eta}_m$ and $\boldsymbol{\nu}_m$, a combination of different complementary filters is able to provide an estimation of the system states such that:

$$\text{If } \left|\boldsymbol{\eta}\text{-}\boldsymbol{\eta}_m\right| < \zeta_\eta \text{ and } \left|\boldsymbol{\nu}\text{-}\boldsymbol{\nu}_m\right| < \zeta_\nu, \exists\left(\boldsymbol{\varepsilon}_\eta, \boldsymbol{\varepsilon}_\nu\right), \text{such that } \tilde{\boldsymbol{\eta}} = \boldsymbol{\eta} - \hat{\boldsymbol{\eta}} < \boldsymbol{\varepsilon}_\eta \text{ and } \tilde{\boldsymbol{\nu}} = \boldsymbol{\nu} - \hat{\boldsymbol{\nu}} < \boldsymbol{\varepsilon}_\eta,$$

that is, the navigation system is exhibiting guaranteed performance. Notice that the condition $\left|\boldsymbol{\eta}\text{-}\boldsymbol{\eta}_m\right| < \zeta_\eta$ imposes the system to be equipped with appropriate sensors, including a device able to provide an estimation of the global position of the system, or at least able to counter-balance the systematic growth of the positioning error, induced by dead-reckoning navigation. As we have already suggested, a solution is to associate with the immerged system a calibrated reference device that is acoustically relaying the GPS information to the system. Being statically immerged, moored, drifting, or actuated, the use of these calibrated references greatly increases the operational and logistic burdens and its efficiency is dependant on the quality of the acoustic link. Terrain-based navigation offers a precious complement of information. Indeed a remarkable terrain feature can be used as a reference point in order to precisely estimate displacement.

Moreover, if this benchmark has been previously spotted and geo-referenced, then terrain navigation offers sufficient information in order to meet the guaranteed performance requirement, by exploiting the geometric and morphological characteristics of the environment; in particular sea bottom features such bathymetry, spatial distribution of biotypes distribution. This technique is named Simultaneous Localisation And Mapping (SLAM) and is currently an active topic of research (Leonard *et al.**, 2002, Nettleton *et al.*, 2000 and Rolfes & Rendas, 2001). The key point here is to guarantee the data association providing an unambiguous recognition of the spotted landmark. This implies to choose features that are robust with respect to the point of view (William *et al.**, 2002), which is a difficult problem. Indeed a wrong data association can drive the vehicle in a situation where it could be lost, justifying the necessity of combining both navigation strategies, using calibrated acoustic relays and terrain-based navigation. Notice that the SLAM aided navigation goal is not to produce a complete and globally consistent map of the environment, but only to provide sufficient environment knowledge in order to estimate, with the desired accuracy, the system displacement. Then the considered maps consist of a few number of relevant spatially features. In this way, the complexity of the filtering / estimation problem is limited and the map-data association is robustly solved (Rolfes & Rendas, 2001). The data-association is generally solved within a stochastic framework, estimating the result of the data association in confronting a representation of the posterior densities to the current sensors information, in order to predict the uncertainty of a given association attempt. *Extended Kalman* and *Monte Carlo* techniques are currently being used to solve this problem (Nieto *et al.*, 2003).

The particular problem of local coordinated navigation of an underwater vehicles flotilla can be elegantly posed using the multi-SLAM technique (Reece & Roberts*, 2005). As for a single vehicle, local coordinated navigation requires the estimation of the necessary information in order to guaranty the movement control of the group. As suggested before, ASC relaying geo-referenced information to the immerged vehicles is greatly helpful. Moreover, since the best communication rate is performed in the vertical water column, this vehicle can also be in charge of insuring the inter-vehicle communication. Nevertheless, the sea surface is not free of obstacle and it is expected that the ASC has to temporarily deviate form its nominal trajectory, thus compromising the communication net. Then, the immerged system has to share other kind of common references. SLAM technique offers interesting alternative to the centralized communication situation, and underlines the problem of extracting terrain-features that are robust with respect to the point of view. The sea bottom, at a given instant is a common reference for all the fleet members, and can greatly helps the relative localisation estimation. This implies that the vehicles are able to exchange information, which could be performed via the surface vessel. An alternative is to use a sub-surface system that can benefit from its vertical actuation in order to avoid obstacle without deviating form its nominal horizontal path. Moreover, this underwater system can adjust its immersion in order to optimize the acoustic cover on top of the flotilla. Nevertheless, despite the poor-rate horizontal communication capabilities, the possibility of a direct communication between two members cannot be neglected. Moreover, a precise temporal synchronization of all the fleet members allows for estimating the distance between the emitter and the receiver. That is precious information concerning the flotilla internal states. Moreover, in this context, an AUV can relay information to another one, which could be unreachable from the (sub-)surface vehicle. Inter-members communication implies to minimize the sum of the necessary information to exchange. In (Lapierre[c] *et al.**, 2003) it has been shown that the collaboration between two underwater vehicles following the same horizontally shifted paths requires, besides the local navigation data, the mutual exchange

of the current control objective of both the vehicles. That is the current path-point each of them is currently tracking. The extension of this solution to N vehicles is still opened. The occurrence on an obstacle induces for the concerned vehicles to deviate from their respective paths. This may imply a reaction on the entire flotilla members, in order to keep the cohesion on the formation and insure a smooth return to a nominal situation. This necessary behaviour requires having regular information about the distance between the vehicles. A robust estimator of these distances has to fuse the (quasi-)global positioning estimation from the (sub-)surface vehicle with the estimation of the relative distance extracted from a measurement of the time-of-flight of the signal along the communication channel. Notice how a precise temporal synchronisation solves trivially the distance estimation. Complementary filters seem to be well suited to this problem, and the guaranteed performance they are offering is of major interest in this application. Fusing all the information related to the acoustical distance between each member towards all, with the one coming from the (sub-)surface vehicle, in considering the erratic sampling rates, is an exciting opened issue.

4. Guidance

The Guidance System processes Navigation/Inertial reference trajectory data and output set-points for desired vehicle's velocity and attitude.

In ROV systems, guidance commands are sent from a ground or mother-boat station, while AUVs have an onboard guidance processor. With regard to this, a guidance system plays the vital role in bringing autonomy to the system (Naeem *et al.*, 2003). The guidance system computes the best approach to be followed by the vehicle, based on the target location, joy-stick operator inputs (if any), external inputs (weather data), Earth topological information, obstacle and collision avoidance data, and finally the state vector which is available as output from the navigation system (Fossen, 2002). Guidance system for underactuated marine vessels is usually used to generate a reference trajectory for time-varying trajectory-tracking or time-invariant manoeuvring for path-following. As a guide-line example, we have chosen to consider the guidance problem for path-following. The underlying assumption in path-following strategy is that the vehicle's forward speed tracks a desired speed profile, while the controller acts on the vehicle orientation to drive it to the path. Thus, as we will see in the sequel, the guidance problem for underactuated vehicles is reduced to the strategy in driving the desired heading angle of the system (ψ_d), while the desired forward velocity (u_d) is left to the arbitrary choice of the mission designer.

4.1 Set-point regulation

A rudimentary guidance system, of general use for marine vessels, is called Set-point regulation. This is a special case where the desired velocity, position, and attitude are chosen to be constant. Applied to a surface craft, the desired attitude is reduced to the desired heading the vehicle has to follow. Then a desired pattern-following (in order to achieve a bottom acoustic coverage for example) will require from the guidance system a collection of n set-points defined by the three following characteristics: desired forward velocity, desired heading and duration, defining an element of the set-point database as: $(U_k \quad \psi_k \quad t_k)^T$, for k=1,…,n. Notice that the environmental information is of major importance for this type of guidance system. Indeed the presence of a lateral current or wind will impact on the system trajectory without being compensated, resulting in a distorted achieved pattern. Nevertheless, this is the simplest guidance, and limited weather

condition is enough to achieve simple missions as acoustic coverage of the seabed, since the acquired data will be post-processed.

4.2 Way-point guidance

Systems for Way-point Guidance are used both for ship and underwater vehicle. The system consists of a way-point generator with the human interface. The selected way-point are defined using Cartesian coordinated $(x_k \quad y_k \quad z_k)^T$ for k=0,…,n, and stored in a way-point database. In the case where the path is only specified in the horizontal plane, only the two coordinates $(x_k \quad y_k)^T$ are used. Additionally, other way-point properties like speed (U_k), heading (ψ_k) etc, can be defined. For surface vessels, this means that the ship should pass through way-point k at forward speed U_k with heading angle ψ_k. The heading is usually unspecified during cross-tracking, whereas it is more important during a crab-wise manoeuvre close to offshore installation, with the condition that the vehicle carries lateral thrusters in order to achieve the dynamic positioning. The way point database can be generated using many criteria, (Fossen, 2002):

- Mission: the vessel should move from some starting point $(x_0 \quad y_0 \quad z_0)^T$ to the terminal $(x_n \quad y_n \quad z_n)^T$, via the way-points $(x_k \quad y_k \quad z_k)^T$.
- Environmental data: information about wind, waves, current can be used for energy optimal routing (or avoidance of bad weather for surface vessels).
- Geographical data: information about shallow waters, islands etc, should be included.
- Obstacles: floating constructions and other obstacles must be avoided.
- Collision Avoidance: avoiding moving vessels close to the defined route by introducing safety margins.
- Feasibility: each way-point must be feasible, in that it must be possible to manoeuvre to the next way-point without exceeding maximum speed, turning rate etc.

On-line replanning can be used to update the way-point database in case of time-varying conditions like changing weather, moving vessels, etc. In practice, the way-point guidance strategy can be cast in the set-point regulation description, in computing the current set-point characteristics in function of the currently tracked way-point k, and the system position, thanks to the following trivial computation:

$$\psi_k = \arctan\left(\frac{x_k - x}{y_k - y}\right) \tag{5}$$

and U_k is left to the arbitrary choice of the operator. This solution constantly adjusts the desired vehicle heading toward the location of the way-point k. This techniques requires the definition of a threshold d_{wp}, under which the vehicle is considered to be in an acceptable vicinity of the way-point k, and allows for iterating the process to the next waypoint k+1.

Another option is to define a followable path, based on the way-point location. It is common to represent the desired path using straight lines and circles arc to connect the way-points (cf. Fig. 5 – dashed line). The drawback of this method, shared by the previous one, is that a jump in the desired yaw-rate r_d is experienced. This is due to the fact that the desired yaw-rate along the straight lines is $r_d=0$ while r_d =constant on the circle arc. Hence introducing a jump in the desired yaw-rate during transition from straight line to circle arc, or between consecutive way-points. This produces a small off-set during cross-tracking.

Cubic spline generated path results in a smoother reference and this drawback is overcome (cf. Fig. 5 – solid line).

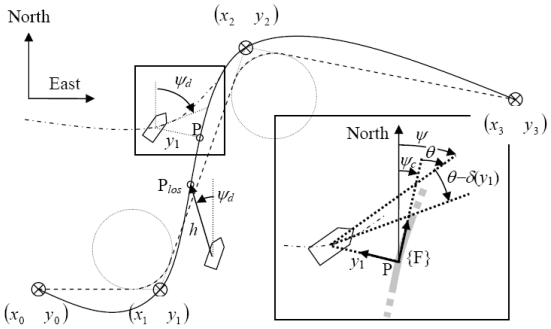

Fig. 5. the path is generated using straight lines and circle arcs – dashed line - or using cubic spline interpolation – solid line. Line of Sight and Nonlinear Approach guidance problem pose.

The path-following guidance strategy requires the definition of a more complex setting, introducing the problem of the path parameterization and the choice of the target-point to be tracked on the path.

4.3 Line of Sight

The Line Of Sight (LOS) strategy is an extension of the way-point guidance described in Equation (5), where the target point is not located onto the next way-point, but defined as the intersection between the path and the LOS vector of length h (horizon). The coordinates $(x_{los} \quad y_{los})$ of the target point P_{los} (cf. Fig. 5) can be easily computed in solving the following equations:

$$(y_{los} - y)^2 + (x_{los} - x)^2 = h^2$$

$$\left(\frac{y_{los} - y_{k-1}}{y_{los} - y_{k-1}}\right) = \left(\frac{y_k - y_{k-1}}{y_k - y_{k-1}}\right) = \text{constant}$$

Notice that this is solvable if and only if $h>y_1$, where y_1 is the cross-tracking error, that is the distance between the robot and the closest point on the path. The two previous equations have two solutions, and a contextual analysis allows for removing this ambiguity.

A more general solution of the guidance problem, originally proposed in (Samson & Ait-Abderrahim, 1991), is the **Nonlinear Approach Guidance** strategy. It is based on the consideration of a Serret-Frenet frame {*F*}, attached to the closest point on the path P. Consider Fig. 5, let ψ_c define the absolute angle of the tangent to the path at point P, and let $\theta = \psi - \psi_c$ be the variable that the control system should reduce to 0 as y_1 vanishes. This desired evolution of θ is captured in the definition of the approach angle $\delta(y_1)$:

$$\delta(y_1) = -\theta_a \cdot \tanh(k_\delta \cdot y_1) \tag{6}$$

where k_δ is a positive gain and $0 < \theta_a \le \pi/2$ defines the asymptotic approach. That is when y_1 is big, the desired angular incidence to the path is θ_a, maximally defined as $\pi/2$ and inducing the desired approach to directly point toward P. As y_1 is reducing $\delta(y_1)$ decreases, down to 0 when

the cross-tracking error is null. This method offers a smooth manoeuvre toward the path and, moreover, defines an appropriate framework in order to derive the control expression using of *Lyapunov* techniques. The global objective of the control is then to reduce the quantity $\theta - \delta(y_1)$ to zero. Nevertheless, this method has a major drawback that consists in the consideration of the closest point P. Indeed, if the system is located the centre of the circle defined by the path-curvature present on the closest point, the guidance definition becomes singular and the ψ_c is no more uniquely defined. This singularity implies a restriction to the domain of validity of the derived control expression, inducing a highly-conservative initial condition $y_1(t=0) < c_{c,\max}^{-1}$, where $c_{c,\max}$ denotes the maximum curvature of the path. This restriction impedes the global nature of guaranteed performance requirement. Nevertheless, this solution stated a theoretical framework that allows for combined guidance / control design process, that will be used in the sequel.

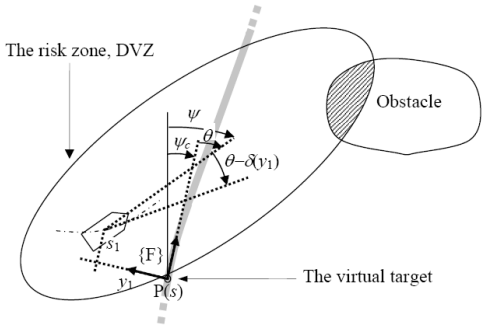

Fig. 6. problem pose for the virtual target principle and the DVZ principle.

4.4 Virtual target vehicle

An alternative to this problem has been originally proposed in (Soetanto *et al.*, 2003 and Lapierre[b] *et al.*, 2006) for an application to wheeled vehicle, extended to marine systems in (Lapierre[a] and Soetanto*, 2006). It consists in the development of the kinematic model of the vehicle in terms of a *Serret–Frenet* frame {*F*} that moves along the path; {*F*} plays the role of the body axis of a Virtual Target Vehicle that should be tracked by the 'real vehicle'. Using this set-up, the cross tracking distance y_1 and the angle $\theta - \delta(y_1)$ become the coordinates of the error space where the control problem is formulated and solved. A *Frenet* frame {*F*} that moves along the path to be followed is used with a significant difference with the previously described nonlinear approach guidance solution: *the Frenet frame is not attached to the point on the path that is closest to the vehicle*. Instead, the origin of {*F*} along the path is made to evolve according to a conveniently defined function of time, effectively yielding an extra controller design parameter $\dot{s}$: where s denotes the curvilinear abscissa of the point P, on the path, thus capturing the evolution of the virtual target along the path (cf. Fig. 6). The consequence is the apparition of another variable s_1, and the control objective is to simultaneously reduce s_1, y_1 and $\theta - \delta(y_1)$ to zero. This seemingly simple procedure allows lifting the stringent initial condition constraint $y_1(t=0) < c_{c,\max}^{-1}$, that arise with the path following controller described in (Samson & Ait-Abderrahim, 1991). The virtual target control law will be derived during the control design, allowing for a solution that exhibits global guaranteed performances.

4.5 Merging other requirements

The previous solutions allow for guiding a marine vehicle toward a desired path. The problem of merging these guidance laws with other requirements, related to obstacle avoidance, environmental effects, optimal route planning, etc. is a difficult subject. Different strategies are proposed, in connection with the criticity of the requirement. For example, the occurrence of an obstacle must induce a rapid reaction, while information about a bad weather present on the current route will imply a path replanning without requiring a reflexive action. Nevertheless, the increasing computing power makes conceivable an obstacle avoidance based on path replanning, so far the obstacle is detected early-enough. The path replanning strategy requires the system to design a safe path between detected obstacles and excluded zones that warrants the vehicle to safely reach the desired goal. The proposed methods are generally classified in two categories: i) Graph Method and ii) Potential Methods. The graph methods are decomposed in two steps: i) the graph construction, allowing investigating all the possible paths and ii) the choice of the optimal path, in concurrently evaluating each of the solution performance (Latombe, 1991). The potential method is based on the space decomposition in terms of fictive potentials. An obstacle or an excluded region will induce a repulsive potential while an attractive potential will be placed onto the goal location. Then searching for the lines of minimum potential allows for planning the possible paths. Analyse of their performances in terms of energy consumption or risks, allow extracting the optimal solution (Barraquand *et al.*, 1992). Nevertheless, these methods do not guarantee the absence of local minima, and the selected path may drive the robot at an undesired impasse (Koditschek 1987). In (Louste & Liégeois, 1998), the authors propose a method based on the *Navier-Stokes* equations of incompressible fluid, undergoing a difference of pressure between the origin and the goal. As the water will always find a way to leak (if possible) form a pressurized confined environment, the analysis of a simulated flow, extracting the routes of maximum fluid particles velocity, allows for finding a global route that travels between obstacles and reach the goal without encountering local minima. Under the assumption that an accurate map of the environment is available; it designs a global solution that guarantees the system to reach the goal, if this solution exists. The problem of coupling this solution with the kinematics requirements of the vehicle is still unsolved. Nevertheless, the simulation of the fluid flow induces heavy computational burden that disqualify this solution in a real time context.

4.6 Reactive obstacle avoidance

A reactive obstacle avoidance strategy will be preferred. This solution is using the Deformable Virtual zone (DVZ, Zapata *et al.*, 2004) principle where a kinematic-dependant potential is attached onto the system, in opposition to the classic potential methods where the map is potentially-active. The idea is to define around the robot a risk zone, the ZVD, in which any obstacle penetration induces a repulsive reaction. The shape of the ZVD is based on an arbitrary choice (generally elliptic), whose parameters are governed by the vehicle kinematics and state evolution. Since the ZVD is attached to the vehicle, both are sharing the same non-holonomic, or underactuated, constraints. The obstacle intrusion is quantified as the area of the penetration (I), cf. Fig. 6. Tedious but straightforward computation yields the jacobian relation between the vehicle velocities (u and r, for unicycle-type robot, $\mathbf{v}$ for marine vehicle) and I. The control design framework is then well posed, and a combined (guidance / obstacle-avoidance / control) design process is possible, in order to seek for solutions that exhibits global guaranteed performances, as detailed in (Lapierre[a] *et al.**, 2006).

The virtual target principle needs to be deeper investigated. An interesting extension is to attribute to the virtual target another extra degree of freedom, y_s. This could allow the point P to leave the path laterally, and design a virtual target control in order to fuse the all the requirements on this runner. Moreover, an adjustment of the s_1 variable will allow for using a second virtual target as a *scout* in order to provide a prediction, compatible with the control theoretical framework.

4.7 Deformable constellation

The consideration of the guidance problem in a multi-vehicles context is an exciting question, where the presence of obstacle in the immediate vicinity of the vehicles is omnipresent. A vehicle deviating from its nominal path may imply a reaction on the entire flotilla members, in order to keep the cohesion on the formation and insure a smooth return to a nominal situation. The principle of the Deformable Constellation, introduced in (Jouvencel *et al.*, 2001), allows for fusing different criteria, related to communication, minimal distance keeping and mission objectives (optimizing the acoustic coverage of the seabed, for example), and attribute to each member the appropriate individual guidance and control instructions. The theoretical framework of this solution needs to be clarified in order to extend its application and evaluate the guaranteed performances of this solution. Based on an extension of the Virtually Deformable zone, this solution allows conceiving the creation of an effective collaborative space, for which the objective of the navigation systems of all the members is to complete the knowledge. In this scope, the constellation guidance is not any more defined around an arbitrary formation, but governed by the obligation of particular measurements, prioritized in function of their necessity. This guidance problem of a flotilla in order to optimize the collaborative acquisition of a desired measurement is a hot topic of research.

5. Control

The Control System generates actuator signals to drive the actual velocity and attitude of the vehicle to the value commanded by the Guidance system.

The control problem is different in function of the system actuation and the type of mission the robot is tasked with. The actuation effects have been considered during the modelling process. While the Navigation system is providing an estimation of the necessary variables, the goal of the guidance system is to take into account the system holonomic property and the type of missions (pose stabilisation / long range routing), in order to cast the control problem under the form of desired values $\boldsymbol{\eta}_d$ and $\boldsymbol{\nu}_d$ to be tracked by $\boldsymbol{\eta}$ and $\boldsymbol{\nu}$, thanks to the control system.

5.1 Hovering

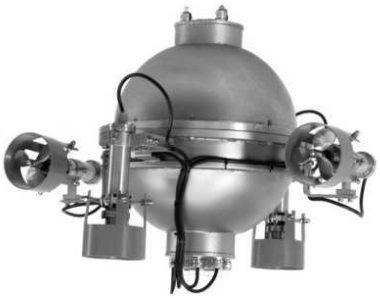

Fig. 7. The URIS ROV, Univerity of Girona, Spain.